PROCEEDINGS OF SCIENCE

The potential role of GRAPES-3 experiment in space weather forecasting

B. Hariharan,[a,*] **M. Chakraborty,**[a] **S.R. Dugad,**[a] **S.K. Gupta,**[a] **Y. Hayashi,**[b] **P. Jagadeesan,**[a] **A. Jain,**[a] **S. Kawakami,**[b] **H. Kojima,**[c] **S. Mahapatra,**[d] **P.K. Mohanty,**[a] **Y. Muraki,**[e] **P.K. Nayak,**[a] **T. Nonaka,**[f] **A. Oshima,**[c] **D. Pattanaik,**[a,d] **M. Rameez,**[a] **K. Ramesh,**[a] **L.V. Reddy,**[a] **S. Shibata**[c] **and M. Zuberi**[a]

[a] *Tata Institute of Fundamental Research, Homi Bhabha Road, Mumbai 400005, India*
[b] *Graduate School of Science, Osaka City University, Osaka 558-8585, Japan*
[c] *College of Engineering, Chubu University, Kasugai, Aichi 487-8501, Japan*
[d] *Utkal University, Bhubaneshwar 751004, India*
[e] *Institute for Space-Earth Environmental Research, Nagoya University, Nagoya 464-8601, Japan*
[f] *Institute for Cosmic Ray Research, Tokyo University, Kashiwa, Chiba 277-8582, Japan*

E-mail: 89hariharan@gmail.com

On 22 June 2015, a massive coronal mass ejection triggered a strong G4 class geomagnetic storm upon arrival at Earth. This weakened the Earth's magnetic shield by allowing the reconnection of the interplanetary magnetic field with the geomagnetic field and resulted in the lowering of the cutoff rigidity for incoming cosmic rays, leading to the production of more muons in the atmosphere by extensive air shower phenomena. The GRAPES-3 muon telescope detected this muon burst (E_μ>1 GeV) which lasted for two hours with an increase of 50 standard deviations in the muon flux, demonstrating a conclusive anti-correlation (CC=–0.94) with B_z. A recent study with data from the scintillator array of GRAPES-3 confirms the increase in muon flux at a level compatible with that of the muon telescope. Unlike the muon telescope, the scintillators record mainly low energy muons (>MeV) and soft components but lack directional information. A well-situated ground based observatory with precise flux measurements irrespective of the energy domain can enable the detection and forecasting of space weather phenomena.

38th International Cosmic Ray Conference (ICRC2023)
26 July - 3 August, 2023
Nagoya, Japan

PoS(ICRC2023)1354

1. Introduction

The Sun is continuously streaming charged particles into the space known as solar wind. When this solar wind reaches Earth, it affects its surroundings such as magnetosphere, ionosphere, thermosphere, exosphere, etc. The amount of energy released from the Sun is known to have certain periodicity of 11 years, termed as solar cycle. This is parameterized by studying the variations by means of sunspots in the Sun's photosphere with telescopes. Sunspot is a darker area due to its relatively cooler temperature (3000–4000 K) than their surroundings (6000 K). The sunspots are associated with intense magnetic field and tends to have eruptions through solar flares and coronal mass ejections (CMEs). Such events are transient in nature and impact the space climate when directed towards Earth. A CME ejects huge amount of plasma from the Sun's corona with a strong magnetic field. When the CMEs are Earth directed, they interact with the geomagnetic field (GMF) and cause geomagnetic storms (GMSs) resulting beautiful phenomena of Aurora Borealis and Aurora Australis in the polar regions. Also, they may disrupt the normal operations of power grids and telecommunication. A notable event called 'Carrington event' occurred on 1–2 September 1859 during solar cycle 10 and is the biggest documented solar storm in the history [1], Another Carrington-like event would cost a devastating damage in global supply chain, power grids, communication satellites, etc [2]. Considering the increasing demand and technological dependence, solar storms and associated effects pose a huge threat to society. A widespread awareness has already emerged and people are preparing to safeguard through the space weather forecast [3–5]. The proposed DISHA H&L is a twin Aeronomy mission with two satellites which are expected to provide valuable insights in modelling ionosphere and thermosphere for better understanding of their role in space weather [5]. Similarly, the planned Aditya-L1 mission will provide solar wind parameters at the first Lagrange (L1) point ($\sim 1.5\times10^6$ km), contemporary to NASA satellites [6].

The WIND and ACE space probes are situated at the L1 point and monitor the Sun's activity. These probes precisely measure important parameters of the plasma namely magnetic field, density, velocity, etc. At Earth, a network of neutron detectors are installed at different geographical locations almost covering entire span of Earth's surface to monitor the Sun's activity [7]. However, no measurements are available during the transport of plasma from L1 to the Earth's surface. On 21 June 2015 there were series CMEs ejected from the Sun. The third CME on 22 June 2015 developed into a G4 class GMS that lowered the cutoff rigidity by magnetic reconnection. This allowed more near-threshold cosmic rays (CRs) to enter into the atmosphere that resulted in more extensive air shower (EAS) production. The GRAPES-3 muon telescope (G3MT) detected excess muons during that time for 2 hours which coincided with the structure of z-component (B_z) of interplanetary magnetic field (IMF) [8]. However, the muon burst was observed after a delay of 32 minutes from the arrival of IMF at L1 and the normal transport time. In a recent study it was found that the array of GRAPES-3 scintillator detectors (G3SD) also recorded a burst of count rates associated with the GMS event on 22 June 2015 after modelling the complex background [9]. Notably the G3SD recorded ~40% higher amplitude compared to G3MT. But the measured amplitude was consistent with the Monte Carlo simulations. Also, the measured delay of 32 minutes in G3SD was found to be same as G3MT. This benchmark event confirms that the amplitude and delay are inherent properties of the GMS. A multi-parameterization study could allow to model the

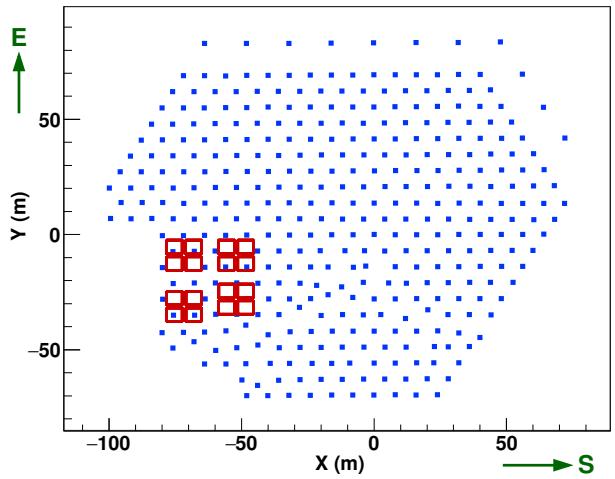

Figure 1: Layout of GRAPES-3 experiment showing (i) array of 400 plastic scintillator detectors (G3SD) and (ii) a large area tracking muon telescope (G3MT).

dependence among the measured parameters at L1 and ground-based CR observatories and leads to a possibility of future space-weather prediction.

2. The GRAPES-3 experiment

The **G**amma **R**ay **A**stronomy at **P**eV **E**nergie**S** – phase **3** (**GRAPES-3**) is a ground-based CR experiment located at Ooty, India (11.4°N, 76.7°E, 2200 m above mean sea level). The GRAPES-3 consists of two detector elements namely (i) an array of 400 plastic scintillator detectors (G3SD) and (ii) a 560 m^2 area tracking muon telescope (G3MT). Each plastic scintillator is made up of four 50×50 cm^2 area plastic scintillators to achieve a sensitive area of 1 m^2. The scintillators are placed with an inter-detector separation of 8 m. The total area covered the G3SD is 25000 m^2. Each scintillator records energy deposit above a certain threshold and relative arrival time of the passing particle with respect to an EAS trigger generated by the G3SD itself. In addition, the scintillator detectors also record the count rates every 100 mS in order to monitor the health of the detectors. Everyday G3SD records about 3.5×10^6 EAS in the energy range of 10^{12}–10^{16} eV. More details about the G3SD can be found here [14].

Proportional counters (PRCs) are the basic building elements of G3MT. Each PRC is a mild-steel tube with a dimension of 600×600×10 cm^3. It has a wall thickness of 2.3 mm. The G3MT consists of sixteen independent muon modules (35 m^2 each) to achieve a total area of 560 m^2. Each muon module has four layers of PRCs arranged in a tightly packed configuration. The layers are sandwiched by 15 cm concrete slabs and alternate layers are placed orthogonal to each other. The PRCs are sealed and filled with P10 gas mixture (90% argon and 10% methane) and applied 3000 V_{DC} for gas ionization. Concrete slabs are placed on top of the top-most PRC layer up to a height of 2 m in an inverted pyramidal shape to provide an energy threshold of sec(θ) GeV with θ<45° in a given projection, yielding a sky coverage of 2.3 sr. The four layer configuration with a layer separation of 52 cm in each projection allows to reconstruct the muons with an angular resolution of 4°. G3MT records PRC hits when an EAS trigger is generated. A separate DAQ

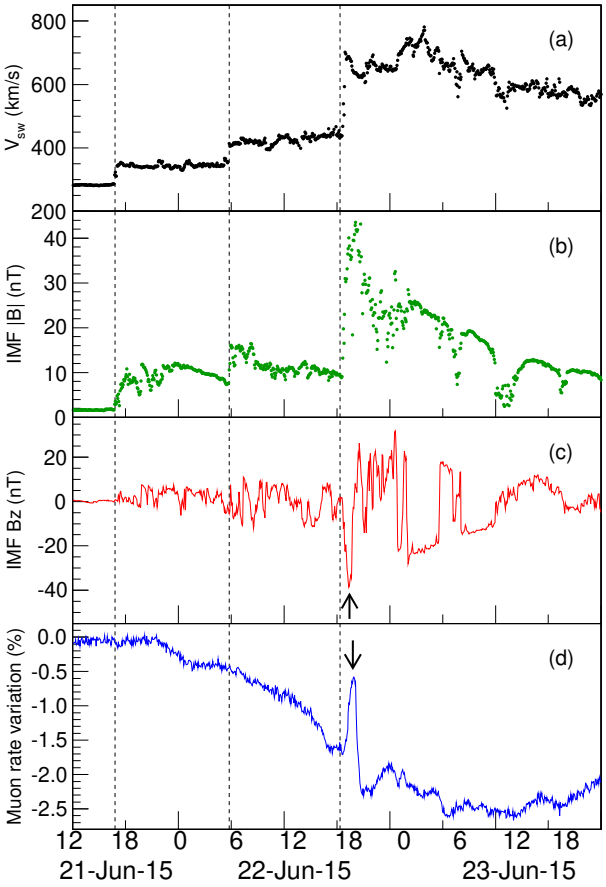

Figure 2: The figures show variation of Solar parameters from WIND spacecraft collected at L1 point, (a) solar wind velocity (V_{SW}), (b) total magnetic field IMF (|B|), (c) IMF B_z, and (d) muon rate measured with G3MT. The X-axis is represented in Universal Time (UT). [Figures are reprodcued from [8]].

records angular muon flux when there is no EAS observation. It also reconstructs the muons into 225 directions and the data recording system bins every 10 sec live time. Everyday G3MT records about 4×10^9 muons above a GeV. More details about the G3MT can be found here [15].

3. Observation of geomagnetic storm events with GRAPES-3

On 21 June 2015, the Sun emitted a series of three CMEs from a sunspot region NOAA 2371. The third episode of CME which arrived on 22 June 2015 exhibited a jump in the solar wind velocity (V_{SW}) to 700 km·sec^{-1} (Figure 2a). On its arrival at Earth's vicinity, it triggered a G4 class GMS which caused Auroras and radio blackouts at many regions. It enhanced the IMF for two hours with a peak magnitude of 44 nT in total IMF (|B|) and –40 nT in B_z (Figures 2a & 2b). These parameters are measured by WIND spacecraft located at L1 point and time shifted to the bow-shock nose, available on OMNIWeb site [6].

As seen in Figure 2d the muon rate initially started to decline slowly after the arrival of the first CME. This is a well-known phenomenon called Forbuse decrease (FD) that causes the slow reduction in the galactic CR intensity. The G3MT recorded a burst of muons for two hours on 22

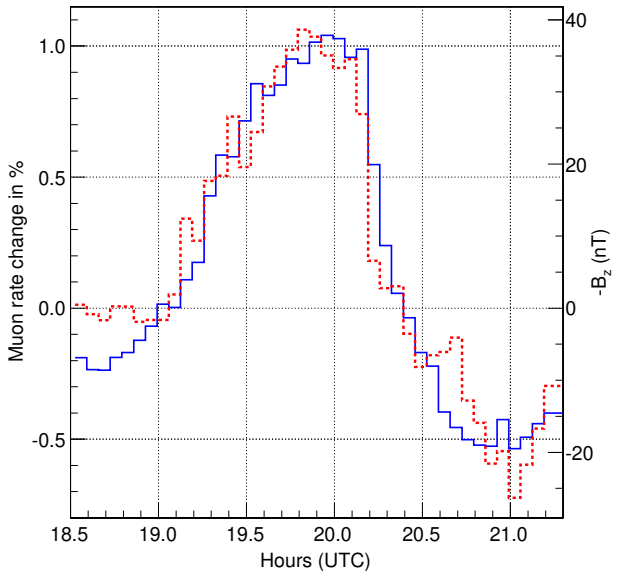

Figure 3: The figure shows the correlation of muon burst and IMF ($-B_z$) with a correlation coefficient of –0.94. [Figure is reproduced from [8]].

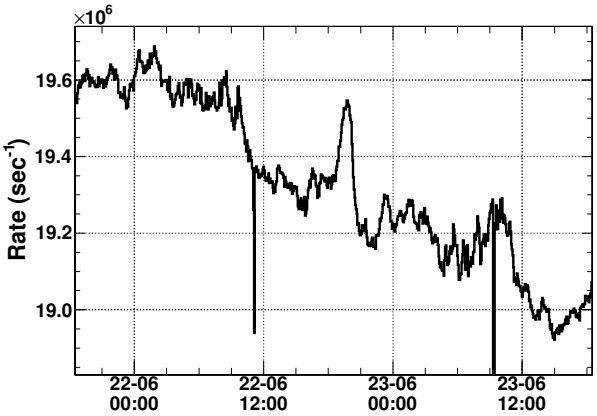

Figure 4: The figure shows background uncorrected count rate of all scintillator detectors combined for 22 June 2015 event. [Figure is reprodcued from [9]].

June 2015 around 18:00 UT after the arrival of third CME. The burst can be seen along with the FD variation. Also, the muon rate is known to have other systematics such as detector efficiency variation, atmospheric pressure variation, and solar diurnal anisotropy (SDA). After removing these systematics, the muon burst was recorded with a peak amplitude of ∼1%, corresponds to 54σ significance. The structure of the muon burst was found to have reasonably good anti-correlation with the magnetic field structure of the IMF (B_z) with the correlation coefficient of –0.94 (Figure 3). This indicates that the magnetic field structure of IMF is responsible for the muon burst. We also found that the muon burst occurred simultaneously in nine directions of G3MT's FOV (13σ significance each), which indicates its origin close to Earth. The interaction of the IMF with GMF caused a temporal magnetic reconnection and reduced the GMF. The reduction in the GMF could result in change in cutoff rigidity for the incoming PCRs. We performed Monte Carlo simulations

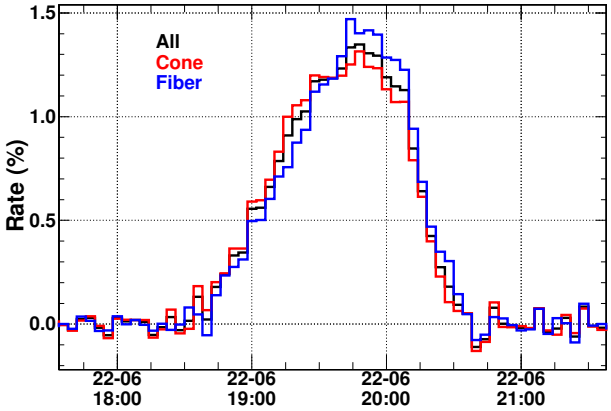

Figure 5: The figure shows background corrected count rates of different detector types namely cone and fiber. The detectors are selected after applying cuts to have less temperature dependence. [Figure is reprodcued from [9]].

using CORSIKA [10] and IGRF-11 [11]. The IGRF provides the GMF for a given location and time. We modified the IGRF model to incorporate the effects of IMF along with GMF. Subsequently, we calculated the resultant cutoff rigidity using backtracing method [12]. The muons ($E_\mu \geqslant 1$ GeV) observed by G3MT are predominantly produced by PCRs in the energy of 10 GeV–10 TeV. The cutoff rigidities for each 4-minute time bin of IMF was used to calculate the muon production using CORSIKA in the above-mentioned energy range. We used in-house detector simulation package to reconstruct the muons into nine directions of G3MT's FOV. We compared the simulated muon profiles with observation in nine directions. The simulated profiles were found to have a reasonably good agreement (correlation of –0.89±0.05). We also found that the muon burst occurred after an additional delay of 32 minutes than the expected from L1 to Earth's surface. A simple model of magnetic reconnection could reproduce the observed muon burst, explained by lowering the cutoff rigidity. The simulations revealed that an enhancement of almost factor 17 in IMF required to reproduce the observed muon profiles of this event. The enhancement (×17) and delay (32 minutes) could be due to compression of IMF during the interaction with GMF. Later studies on the same event showed that the muon burst was accompanied by a interplanetary anisotropy [13]. This analysis was carried out by re-binning of G3MT's FOV into nine North-South oriented strips as shown in Figure 1 of [13]. The anisotropy structure was found to be time-shifted from East to West, also to be rigidity dependent, whereas, the muon burst occurred in all nine strips simultaneously. The global neutron monitor network detectors failed to resolve these distinct features due to their limited sensitivity.

The G3SD is primarily designed to record first arrival time and total energy deposit of CR secondaries for each EAS trigger. Unlike G3MT, the G3SD is being operated at a lower threshold corresponding to a few MeV. As mentioned in the previous section, the G3SD is also equipped with an additional DAQ to count the pulses every 100 ms. Since the observation of muon burst was demonstrated to be due to lowering of cutoff rigidity for PCRs in the energy range of 10 GeV–10 TeV, it is possible to observe this phenomenon using G3SD. Each scintillator detector has a count rate of about 200–300 sec^{-1}. Figure 4 shows the combined count rates of all scintillator detectors for

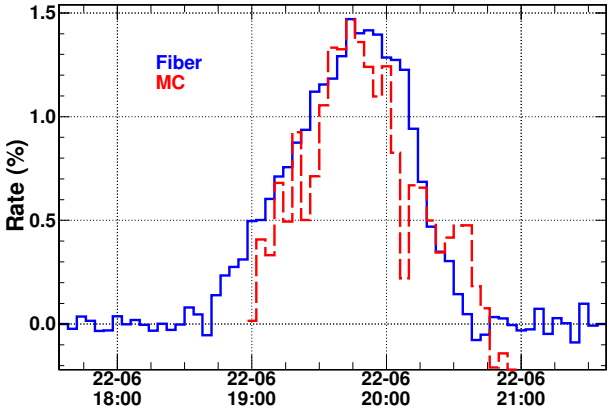

Figure 6: The figure shows background corrected rate of fiber type scintillator detectors compared with Monte Carlo simulations. [Figure is reprodcued from [9]].

22 June 2015 event. A burst-like structure can be seen in the count rate variation along with a FD decrease. It is to be noted that the profile also contains many transitory variations which are due to temperature effects of photomultipliers used. We quantitatively selected the scintillator detectors having less temperature dependence using stringent cuts. Savitzky–Golay filter was used to model the FD and background subtraction. Figure 5 shows the background corrected count rates for the selected detectors for different detector types employed in GRAPES-3 namely cone and fiber. The burst-like structure was found to have excess count rates, corresponds to more than 100σ for cone and fiber detector rated combined. It is interesting to note that the scintillator count rates recorded a peak amplitude of ∼1.4% for fiber detectors, which is ∼40% higher than G3MT. However, the enhancement of the IMF and delay remain unchanged. Figure 6 shows the background corrected count rate for the fiber detectors compared with Monte Carlo simulations. The simulation conditions of scintillator detectors were kept same as G3MT. A reasonably good agreement between these two profiles can be seen. The Monte Carlo simulations also revealed that the scintillator rate composes of 58% muons, 11% gamma, 29% electrons, and the remainder hadrons. Since the G3SD do not record the direction of the passing particles, the anisotropy feature seen by [13] could not be resolved here. Also, this could be the reason for small broadening of the signal when compared with Monte Carlo simulations (Figure 6).

4. Conclusion

Satellite probes at L1 provide valuable information about solar wind parameters. The planned and proposed future missions of Aditya-L1 and DISHA H&L are expected to play crucial roles in understanding solar storms and modelling of Earth's ionosphere. The studies carried out by using G3MT [8, 13] and G3SD [9] on 22 June 2015 event confirm that the GMS arrived from L1 to Earth's surface after a delay of 32 minutes than expected. Monte Carlo simulations also confirm that an enhancement of ×17 in the IMF is required to reproduce the observed muon burst on 22 June 2015 in both the instruments. Further studies on similar events from archival data revealed that the delay and enhancement of IMF are inherent properties of the GMS borne out by the magnetic reconnection. There Information are essential for space weather in forecasting of future solar storms. Hence, the

GRAPES-3 detectors can contribute to the space weather in different energy domains and provide valuable information during the transit of GMS from L1 to Earth's surface.

5. Acknowledgements

We are grateful to D.B. Arjunan, A.S. Bosco, V. Jeyakumar, S. Kingston, N.K. Lokre, K. Manjunath, S. Murugapandian, S. Pandurangan, B. Rajesh, R. Ravi, V. Santhoshkumar, S. Sathyaraj, M.S. Shareef, C. Shobana, and R. Sureshkumar for their role in efficient running of the experiment. We acknowledge support of the Department of Atomic Energy, Government of India, under Project Identification No. RTI4002. This work was partially supported by grants from Chubu University, Japan.

References

[1] R.C. Carrington, Monthly Notices of the Royal Astronomical Society, 20 (1859) 13–15.

[2] "http://www.express.co.uk/news/science/1134601/nasa-solar-storm-carrington-event-kepler-satellite-loeb-oumuamua-space-news"

[3] "https://obamawhitehouse.archives.gov/blog/2016/10/12/preparing-nation-space-weather-new-executive-order"

[4] A. Bhardwaj et al., Space Weather, 14(12), 2016, 1082–1094.

[5] Annual Report, 2019–2020.

[6] "http://omniweb.gsfc.nasa.gov/form/omni_min.html"

[7] "https://www.nmdb.eu"

[8] P.K. Mohanty et al., Phys. Rev. Lett. 117 (2016) 171101.

[9] B. Hariharan et al., Journal of Atmospheric and Solar–Terrestrial Physics 243 (2023) 106005.

[10] "https://www.ikp.kit.edu/corsika"

[11] C. Finlay, Geophys. J. Int. 183 (2016) 1216.

[12] D.F. Smart, D.F. and M.A. Shea, M. A., Final Report, Grant NAG5–8009.

[13] P.K. Mohanty et al., Phys. Rev. D, 97 (2017) 082001.

[14] S.K. Gupta et al., Nuclear Instruments and Methods in Physics Research A, 540 (2005) 311-323.

[15] Y. Hayashi et al., Nuclear Instruments and Methods in Physics Research A, 545 (2005) 643-657.

[16] M. Zuberi et al., Proceedings of Science PoS(ICRC2017)302.